Title

Pharmacological inhibition of S-nitrosoglutathione reductase improves endothelial vasodilatory function in rats in vivo

Journal

Journal of Applied Physiology, 114(6)

ISSN

8750-7587

Authors

Chen, Qiumei
Sievers, Richard E
Varga, Monika
et al.

Publication Date

2013-03-15

DOI

10.1152/japplphysiol.01302.2012

Peer reviewed

Articles in PresS. J Appl Physiol (January 24, 2013). doi:10.1152/japplphysiol.01302.2012

JAPPL-01302-2012R1 Corrected Fig 3 legend 1-12-13

Pharmacological Inhibition of S-Nitrosoglutathione Reductase Improves Endothelial Vasodilatory Function in Rats *in vivo*

Qiumei Chen*, Richard E. Sievers[§], Monika Varga*[1], Sourabh Kharait[#], Daniel J. Haddad*[2], Aaron K. Patton[‡], Christopher S. Delany[‡], Sarah C. Mutka[‡], Joan P. Blonder[‡], Gregory P. Dubé[‡3], Gary J. Rosenthal[‡], and Matthew L. Springer*[§†]

*Cardiovascular Research Institute, [§]Division of Cardiology, [#]Division of Nephrology, and [†]Eli & Edythe Broad Institute of Regeneration Medicine and Stem Cell Research, University of California, San Francisco, San Francisco, CA; and [‡]N30 Pharmaceuticals, Boulder, CO

Current affiliations: [1]Stryker Corporation, Fremont, CA; [2]University of Vermont College of Medicine, Burlington, VT; [3]OPK Biotech, LLC, Cambridge, MA

Chen: GSNOR inhibition improves endothelial function

Correspondence to:
Matthew L. Springer
Division of Cardiology, Box 0124
University of California, San Francisco
San Francisco, CA 94143-0124
415-502-8404 (Telephone)
matt.springer@ucsf.edu

AUTHOR CONTRIBUTIONS

Participated in research design: Chen, Sievers, Kharait, Blonder, Mutka, Dubé, Rosenthal, and Springer
Conducted experiments: Chen, Sievers, Varga, Kharait, Haddad, Patton, Mutka, and Delany
Contributed new reagents or analytic tools: Blonder, Patton, and Mutka
Performed data analysis: Chen, Haddad, Kharait, Patton, Mutka, and Blonder
Wrote or contributed to the writing of the manuscript: Chen, Mutka, Blonder, Dubé, Rosenthal, and Springer

ABSTRACT

Nitric oxide (NO) exerts a wide range of cellular effects in the cardiovascular system. NO is short-lived, but S-nitrosoglutathione (GSNO) functions as a stable intracellular bioavailable NO pool. Accordingly, increased levels can facilitate NO-mediated processes, and conversely, catabolism of GSNO by the regulatory enzyme GSNO reductase (GSNOR) can impair these processes. Because dysregulated GSNOR can interfere with processes relevant to cardiovascular health, it follows that inhibition of GSNOR may be beneficial. However, the effect of GSNOR inhibition on vascular activity is unknown. To study the effects of GSNOR inhibition on endothelial function**,** we treated rats with a small-molecule inhibitor of GSNOR (N6338) that has vasodilatory effects on isolated aortic rings and assessed effects on arterial flow-mediated dilation (FMD), an NO-dependent process. GSNOR inhibition with a single i.v. dose of N6338 preserved FMD (15.3±5.4% vs. 14.2±6.3%, P=NS) under partial NOS inhibition that normally reduces FMD by roughly 50% (14.1±2.9% vs.7.6±4.4%, P<0.05). In hypertensive rats, daily oral administration of N6338 for 14 days reduced blood pressure (170.0±5.3/122.7±6.4 mmHg vs. 203.8±1.9/143.7±7.5 mmHg for vehicle, P<0.001) and vascular resistance index (1.5±0.4 mmHg·min/L vs. 3.2±1.0 mmHg·min/L for vehicle, P<0.001), and restored FMD from an initially impaired state (7.4±1.7% day 0) to a level (13.0±3.1% day 14, P<0.001) similar to that observed in normotensive rats. N6338 also reversed the pathological kidney changes exhibited by the hypertensive rats. GSNOR inhibition preserves FMD under conditions of impaired NO production and protects against both microvascular and conduit artery dysfunction in a model of hypertension.

KEYWORDS–hypertension, flow-mediated vasodilation, nitric oxide, S-nitrosoglutathione, S-nitrosoglutathione reductase

Nitric oxide (NO) has emerged as a key player in the cardiovascular system, mediating diverse physiological processes including vasodilation (31, 33, 41). Many effects of NO are mediated by the transfer of an NO group to cysteine sulfhydryls on proteins via S-nitrosylation (35), a process that plays an important role in many NO-dependent cardiovascular processes (20) and causes significant protein modification within endothelial cells (43). NO is short-lived, but exists physiologically in other forms like nitrite, nitrate, and S-nitrosothiols (SNOs), which include S-nitrosylated cysteine residues in serum proteins, and S-nitrosoglutathione (GSNO) in the cytoplasm. In particular, GSNO is thought to serve as an important intracellular bioavailable NO pool, which is in equilibrium with other intracellular SNOs that facilitate transnitrosylation (NO transfer between proteins) (12, 18). Accordingly, increased levels of GSNO can facilitate NO-mediated processes, and conversely, catabolism of GSNO by GSNO reductase (GSNOR), a regulatory enzyme that degrades GSNO and is thought to be the main regulator of GSNO levels in vivo (22), can impair these processes. This premise is supported by the observations that in human asthma, GSNOR regulates airway SNO content and hyperresponsiveness (29, 30), and GSNOR-deficient mice are protected from airway hyperresponsiveness in an asthma model (28).

Because dysregulated GSNOR can reduce levels of GSNO and can interfere with processes relevant to cardiovascular health, it follows that GSNOR inhibition may be beneficial in certain situations. GSNOR inhibition promotes vasorelaxation of isolated aortic rings (32) and genetic deletion of GSNOR lowers systemic vascular resistance and improves post-infarction myocardial perfusion (21, 23), although complete deletion also lowers cardiac contractility (4). Together, these observations suggest that GSNOR is highly relevant to the cardiovascular system and that inhibition under appropriate circumstances could provide therapeutic strategies for various forms of cardiovascular disease.

One effective way to assess vascular health in humans is to measure the vasodilation of arteries in response to increased blood flow, a process called flow-mediated (vaso)dilation (FMD) (6). Transient occlusion of the brachial artery with a blood pressure (BP) cuff and subsequent release result in reactive hyperemia and vasodilation, which is measured by ultrasound detection of arterial diameter before and after occlusion. The resulting FMD is primarily NO-mediated (14), which is demonstrable through inhibition of NO synthase (NOS) by inhibitors such as N^G-monomethyl-L-arginine (L-NMMA). This effect relies on functional endothelium to sense fluid shear stress, activating endothelial NOS (eNOS) to produce NO, which diffuses to and relaxes the underlying smooth muscle. FMD has become widely accepted as a biomarker of endothelial function and cardiovascular health (2, 11, 40).

We developed an approach to measure FMD in the femoral artery of living rats that is functionally analogous to brachial artery FMD measurement in humans (17). This system holds a substantial advantage over measurement of vasorelaxation of isolated aortic segments because it reflects intact physiology and is analogous to the clinically-measured effect. Using this system, we show here that a novel small-molecule reversible inhibitor of GSNOR, N6338 (36), not only preserves FMD in models of endothelial dysfunction, but also lowers BP and vascular resistance in hypertensive rats.

METHODS

Animals

Unless otherwise indicated, Sprague-Dawley and Dahl-S rats (Charles River, Wilmington, MA) were 12 or 9 weeks of age, respectively, at the initiation of N6338 treatment. Sprague-Dawley rats were fed standard diet (Purina, Richmond, IA) while Dahl-S rats were fed low-salt (0.26%

NaCl) or high-salt (4% NaCl) diet to induce a normotensive or hypertensive phenotype, respectively. 9-week old Dahl-S rats were delivered to UCSF after 3 weeks on the high- or low-salt diet. Dahl-S rats are normotensive on low salt diet and hypertensive on high salt diet, but a minority will not become hypertensive on high salt so screening is a traditional step. Indeed, we found that a small number of rats on low salt spontaneously became hypertensive. Therefore, an excess of Dahl-S rats were fed the appropriate diets during the initial 3 week period. BP was subsequently measured via tail cuff, and only those on high-salt with stable hypertension (n=14) and those on low salt with stable normal BP (n=12) were randomized into drug or control groups for further use on day 0 (D0). The diets were maintained through the end of study (D14). For another experiment, the rats were all delivered before the switch from low to high salt diet so that baseline BP could be measured before switching all rats to high salt diet. BP was read again after 3 weeks and any rats that had not converted to hypertension were removed. The remaining rats were randomized into drug (n=10) or vehicle (n=7) groups, with the rats serving as their own normotensive controls based on their baseline BP. Despite differences in the delivery schedule of the rats in the two BP experiments, the two experiments did not differ with respect to the switch from low- to high-salt and the treatment with the drug. All experiments were approved by the UCSF Institutional Animal Care and Use Committee.

GSNOR inhibition in vitro

N6338 (N30 Pharmaceuticals, Boulder, CO) and GSNOR (Emerald BioStructures, Bainbridge Island, WA) were prepared as previously described (36). The potency of N6338 inhibition of GSNOR activity was determined *in vitro* via determination of the N6338 concentration that inhibited maximal GSNOR activity by 50% (IC_{50}). Final assay conditions were 0.5 μg/mL

GSNOR, 240 μM GSNO, and 300 μM NADH in 100 mM sodium phosphate buffer, pH 7.4 at 25˚C. N6338 concentrations ranged from 0-2 μM. Reaction volumes were 300 μL in a UV transparent 96-well plate (Costar 3635). The change in absorbance at 340 nm (from oxidation of NADH to NAD^+) was followed for 3 min in a SpectraMax M2 plate reader. The initial linear reaction rate (mAU_{340}/min) was plotted against inhibitor concentration and fit to a sigmoidal dose-response model (variable slope) using GraphPad Prism 5 software.

GSNOR immunohistochemistry

Formalin fixed, paraffin embedded tissues from Dahl-S study rats (normal diet vehicle control group) were stained with a rabbit polyclonal GSNOR antibody (11051-1-AP, Proteintech, Chicago, IL). Commercially available human tissues (tissue source for Figure 1C,D from Premier Laboratories, Longmont, CO; for 1E from Folio Biosciences, Columbus, OH) were stained with a monoclonal anti-GSNOR antibody (N30-C3) raised in a rat immunized with full length human GSNOR protein at ProMab Biotechnologies (Richmond, CA) for N30 Pharmaceuticals. Slides were deparaffinized in xylene and rehydrated to water though a series of alcohol gradients. The slides were pretreated in a 95˚C citrate pH 6.1 antigenic retrieval solution (Dako, Carpinteria, CA). After allowing the slides to cool to room temperature, a 3% hydrogen peroxide solution (EMD Chemicals, Gibbstown, NJ) was added to quench endogenous peroxidase activity. Slides were preincubated with Serum Free Protein Block (Dako), followed by incubation with the GSNOR antibody or a non-specific rat IgG control (AbD Serotec, Raleigh, NC) or rabbit Ig fraction (Dako). Human tissue slides were then incubated with rabbit anti rat immunoglobulin (Dako), and both human and rat tissues were labeled with a goat anti

rabbit polymer (Dako). DAB+ (Dako) was used for detection and slides were counter-stained with hematoxylin (Dako).

GSNOR activity

Hearts and aortas from male Sprague-Dawley rats (Harlan, Indianapolis, IN, 8-10 weeks of age, weighing 250-300 g) were frozen in liquid nitrogen and stored at -70˚C. Tissues were pulverized to powder in liquid nitrogen and then homogenized in 50 mM Tris-HCl (pH 7.4), 250 mM NaCl, 0.1 mM DTPA, 10 mM NEM, 1% igepal CA-630, with complete, EDTA-free, protease inhibitor cocktail (Roche Diagnostics, Mannheim, Germany). Homogenates were clarified by centrifugation and total protein determined by the bicinchoninic acid method. Tissue homogenates (4.4 mg/mL total protein) were diluted 10-fold into reaction buffer (100 mM sodium phosphate pH 7.4 and 250 μM NADH). GSNO-dependent NADH depletion was determined spectrophotometrically by measuring change in absorbance at 340 nm for 3 min at 20˚C in the absence and presence of 250 μM GSNO. Additions of N6338 to reactions containing GSNO were as indicated in the text.

Measurement of nitrosated species (SNOs)

Mouse embryonic fibroblast cells (a generous gift from Limin Liu, UCSF) were immortalized with SV-40 T-antigen (Applied Biological Materials, Richmond, BC, Canada). The cells were cultured in 6-well plates at 1-2x10^6 cells/well and grown overnight in DMEM supplemented with 10% FBS, 100 U/mL penicillin, 100 μg/mL streptomycin, and 2 mM glutamine. Media was replaced with fresh DMEM with 500 μM GSNO (N30 Pharmaceuticals) and either vehicle or 50 μM N6338 and incubated for 4 hours. Nitrosylated species were quantitated using the triiodide

based chemiluminescence method as described (32) with the following modifications. Cells were washed in PBS and collected into lysis buffer (50 mM NEM, 50 mM potassium phosphate pH 7.0, 5 mM DTPA, 0.2 mM neocuproine, 20 mM ferricyanide, and 1% Igepal CA-630). Cell lysates were treated with 15% v/v of a sulfanilamide solution (5% w/v in 0.3 M HCl) and the triiodide reaction was performed at room temperature using GSNO to generate a standard curve.

Aortic ring relaxation assay

Aortic rings from male Sprague Dawley rats (Harlan) were mounted at isometric tension in a small vessel wire myograph (DMT 610M, DMT-USA, Atlanta, GA) in Krebs bicarbonate buffer containing 119 mM NaCl, 4.7 mM KCl, 1.2 mM $MgSO_4$, 1.2 mM KH_2PO_4, 2.5 mM$CaCl_2$, 25 mM $NaHCO_3$, 0.03 mM EDTA, and 5.5 mM glucose and continuously gassed with 95% O_2: 5% CO_2. Rings were equilibrated at a resting tension of 2 g for one hour and then treated with 10 μM 1H-[1,2,4] oxadiazolo [4,3-a]quinoxalin-1-one (ODQ, a guanylate cyclase inhibitor), 100 μM L^G-monomethyl-arginine (L-NMMA, a NOS inhibitor), or 300 μM 2-(4-carboxyphenyl)-4,5-dihydro-4,4,5,5-tetramethyl-1H-imidazolyl-1-oxy-3-oxide (carboxy PTIO; an NO scavenger) for 30 min. Control aortas were treated with vehicle (water). Aortas were then pre-contracted with 0.5 μM phenylephrine (EC85). After a plateau of phenylephrine effect was achieved, N6338 was added in half-log cumulative doses ranging from 1 μM to 1 mM. Data was acquired and analyzed using Powerlab software (ADInstruments, Colorado Springs, CO). Additional data analyses were performed in GraphPad Prism. The amount of relaxation was reported as the percent of maximum relaxation.

Inhibition of GSNOR and NOS in vivo

Acute GSNOR inhibition *in vivo* was achieved by i.v. injection of N6338 (10 mg/kg in 0.1 ml saline/100 g). Sub-chronic GSNOR inhibition *in vivo* was achieved by daily oral administration of 10 mg/kg/day N6338 prepared in 0.5% wt/vol carboxymethylcellulose. Inhibition of NOS was achieved by i.v. injection of L-NMMA (5 mg/kg in 0.1 ml saline/100 g).

Measurement of FMD

FMD was measured in living rats as described previously (17). Briefly, an arterial loop occluder was surgically positioned upstream of the femoral artery and passed through 15 cm PE-90 tubing. After a 15 minute equilibration, the artery was occluded for 5 min followed by reperfusion of the leg. Femoral artery diameter was measured with a 35 MHz ultrasound transducer (Vevo660, VisualSonics, Toronto) over 3 min. Image analyses were performed offline from recorded loops using an automated system (Brachial Analyzer 5, Medical Imaging Applications, Coralville, IA) (17). Volumetric flow was calculated as π x (diameter/2)^2 x mean flow velocity (V). V was calculated as velocity-time integral x duration of heart cycle. All diameter readings were taken at diastole, and flow velocity represents the mean angle-corrected Doppler-flow velocity. FMD was calculated as % change: (peak diameter$_{postischemia}$ − diameter$_{baseline}$)/ diameter$_{baseline}$ x 100, and presented both as raw data and indexed to wall shear rate (WSR) by calculating FMD/WSR. WSR was calculated as 4 x velocity/diameter at peak response. We used WSR rather than wall shear stress, which also depends on blood viscosity, under the assumption that blood viscosity was constant.

BP and vascular resistance index detection

BP was measured using a noninvasive, computerized piezoplethysmography tail-cuff system (ML125/R NIBP; ADInstruments, Colorado Springs, CO). The investigator taking BP measurements was blinded to treatment, but not blinded to diet (high- vs. low-salt) for technical reasons; the investigator measuring FMD and flow velocity was blinded to treatment and diet. Because tail cuff methodology yields only approximations of diastolic BP based on systolic BP measurements, vascular resistance was expressed as an index calculated as √(diastolic pressure approximation x systolic pressure) / volumetric blood flow (7).

Kidney histology

Kidneys and hearts were wet-weighed and snap-frozen in liquid nitrogen. Superficial renal sections (10 microns) were stained with hematoxylin and eosin and examined histologically by a blinded examiner.

Molecular assays in aortic extracts

cGMP was analyzed from homogenized aorta samples from the N6338- and vehicle-treated high-salt groups using a colorimetric Enzyme Immunoassay cGMP kit (Cayman, Ann Arbor, MI) according to the manufacturer's instructions.

Statistics

For aortic ring relaxation, statistical analysis was performed using GraphPad Prism and significant differences among groups were determined via two-way ANOVA with treatment and dose as factors, followed by Bonferroni's post-hoc correction for multiple comparisons. Statistical analysis was performed using one-way ANOVA for weight comparisons, two-way

ANOVA for aortic ring relaxation measurement, and two-way repeated measures ANOVA for the acute FMD suppression study and for BP and FMD comparison in the chronic study with GraphPad Prism, followed by Bonferroni post hoc correction with significance adjusted for multiple comparisons where appropriate. Single comparison between all untreated (day 0) Dahl-S rats on high salt vs. low salt in the chronic study was performed by Student's t-test. For vascular resistance index, a two-way repeated measures ANOVA was performed with main factors salt level and treatment, and planned pairwise comparisons were tested using linear contrast statements with significance determined using Bonferroni adjustment for multiple comparisons. Analyses were performed using Statistica (v6.0, StatSoft, Inc). Statistical significance was determined after adjusting for multiple comparisons to maintain the overall alpha error rate of $P<0.05$.

RESULTS

N6338 is a GSNOR inhibitor

N6338 caused dose-dependent, potent inhibition of human GSNOR activity *in vitro* (Figure 1A), and increased the level of SNOs in cultured mouse embryonic fibroblasts (Figure 1B).

GSNOR expression in the vasculature

GSNOR protein expression was detected in vascular tissue by immunohistochemistry. Antibodies against human (Figures 1D, E) or rat (Figure 1G) GSNOR demonstrated the presence of GSNOR in small macrovessels in human and rat heart tissue sections. In both species, arterioles and presumably small arteries showed prominent GSNOR immunostaining in smooth muscle, but little, if any, staining in endothelium (Figure 1D, G). In a human venule, GSNOR

271 staining was apparent in endothelium (Figure 1E). GSNOR was also prominently expressed in
272 human cardiomyocytes (Figure 1E). Consistent with the results in human tissue, faint staining
273 was observed in rat cardiomyocytes (Figure 1G). No staining was evident in human (Figure 1C)
274 or rat (Figure 1F) heart sections stained with the respective IgG negative control.
275
276 *GSNOR activity in cardiovascular tissues*
277 GSNOR enzyme activity was measured in rat heart and aorta homogenates to further identify the
278 presence of GSNOR in vascular tissue. GSNOR activity was detected in homogenates from both
279 rat aorta and heart (Figure 1H). N6338 inhibited this enzyme activity when added *in vitro*.
280 Specifically, N6338 decreased GSNOR activity by 73.3 ± 8.5% (heart) and 85.3 ± 17.7% (aorta)
281 at 1 μM N6338, and by 90.8 ± 1.5% (heart) and 94.5 ± 6. 2% (aorta) at 10 μM N6338.
282
283 *N6338 causes relaxation of preconstricted aortic rings in vitro*
284 To further demonstrate that GSNOR inhibition by N6338 can directly influence vascular tone,
285 the effects of N6338 were tested in isolated aortic rings. N6338 caused a dose-dependent
286 relaxation in rat aortic rings that had been precontracted with phenylephrine (Figure 1I). To
287 determine whether this relaxation was NO-dependent, reagents affecting various pathways of
288 NO-mediated relaxation were added prior to the phenylephrine and N6338 additions. Incubation
289 of rings with either soluble guanylate cyclase inhibitor ODQ, NOS inhibitor L-NMMA, or NO
290 scavenger carboxy PTIO significantly attenuated N6338 (1 to 100 μM) relaxation compared to
291 vehicle-treated control rings, demonstrating the dependence of N6338's effects on the classical
292 NO/cGMP mechanism for smooth muscle relaxation.
293

GSNOR inhibition prevented impairment of FMD caused by partial inhibition of eNOS

We first determined whether a single dose of GSNOR inhibitor could preserve FMD under conditions of partial NOS inhibition. Rats were injected i.v. with PBS (negative control) or N6338 (10 mg/kg in 0.1 ml saline/100 g) followed by 300 µl PBS to flush the infusion system. After 24 hours, we measured FMD and then administered 5 mg/kg of the NOS inhibitor L-NMMA, a dose that we had previously determined to inhibit FMD by approximately 50% (Q.C., unpublished). FMD was measured again 10 min after L-NMMA. We used a cross-over design in which rats were randomly split into two groups (n=7/group), with one group given N6338 and the other group given PBS. After a 2 week wash-out period, the groups were reversed and received the opposite treatment. As shown in Figure 2, FMD responses 24 h after treatment with PBS or N6338, but before L-NMMA, were similar, indicating that GSNOR inhibition has little or no effect on FMD in normal arteries. However, while L-NMMA significantly reduced FMD in PBS-treated rats (14.1±2.9% vs. 7.6±4.4%, $P<0.05$), there was no significant difference in FMD before and after L-NMMA in N6338-treated rats (15.3±5.4% vs. 14.2±6.3%, P=NS). There was also a significant difference between post-L-NMMA FMD in the PBS-treated vs. N6338-treated rats (7.6±4.4% vs. 14.2±6.3%, $P<0.05$). Calculation of FMD relative to WSR (FMD indexed to WSR) resulted in similar relationships. Femoral artery diameter was not significantly decreased by L-NMMA before or after occlusion in each group (data not shown). These results demonstrate that N6338 prevented the reduction in FMD that would have otherwise occurred following administration of L-NMMA.

GSNOR inhibition reduced BP in Dahl-S hypertensive rats

We then asked if it is possible to recapitulate decreased FMD in an inflammation-based chronic

hypertension model, the Dahl-S rat maintained on a high-salt diet, and whether inhibition of GSNOR could reduce BP and restore FMD in this model. N6338 in a solubilization vehicle (0.5% wt/vol carboxymethylcellulose) was delivered orally at 10 mg/kg/day once daily, beginning at day 0; control groups received only vehicle. Hypertensive and normotensive rats had been previously randomized to groups after the initial BP measurement.

As shown in Figure 3A and with exact values shown in Table 1 (due to the complexity of the data), at D0, D4, D9, and D14, systolic BP and diastolic BP measured by tail cuff under anesthesia did not differ between the low-salt groups treated with vehicle vs. drug, showing that the GSNOR inhibitor did not affect BP in healthy animals. (Note that diastolic BP values resulting from tail cuff measurements are approximations based on the systolic measurements, but are presented for reference.) BP in the high-salt vehicle group was substantially higher than BP in the low-salt groups ($p<0.05$ overall), confirming that this rat model of vascular disease successfully manifested a disease state similar to that of hypertensive humans.

While the overall F-test was significant, specific inter-group comparisons failed to retain significance after adjusting the alpha error rate for multiple comparisons in the anesthetized animals. For this reason, and because anesthetized conditions result in abnormally low BP especially as measured with tail cuff methodology, we performed a similar experiment in which BP was measured in conscious Dahl-S rats acclimated to the procedure with exact values shown in Table 2. Notably, in the high-salt drug group, BP was initially high, but decreased significantly over time and was substantially lower by D9 and D14; demonstrating a BP-lowering effect of the GSNOR inhibitor in hypertensive, but not normotensive, Dahl-S rats (Figure 3B). (The subsequent results presented below derive from the rats in which BP had been measured under anesthesia.)

GSNOR inhibition reduced vascular resistance in Dahl-S hypertensive rats

Measuring vascular resistance provides a more reliable indication of microvascular tone than assessing BP alone. To determine if GSNOR inhibition protects microvascular function in Dahl-S hypertensive rats, we calculated a vascular resistance index using the systolic BP measurements and the diastolic BP approximations (see Methods) at both baseline (i.e., prior to femoral artery occlusion) and at peak blood flow during reactive hyperemia. This provides an indication of the extent to which chronic GSNOR inhibition impacts microvascular tone at "rest" and under near maximal dilatory conditions in a disease state with increased microvascular resistance.

As shown in Figure 4, in general, post-occlusion vascular resistance relationships mirrored pre-occlusion relationships, but significance was stronger for the post-occlusion numbers, and strongest at D14. At D0, post-occlusion vascular resistance index trended higher in the high-salt groups than in the low-salt groups (vehicle groups at 3.7±1.8 vs. 1.6±0.4 mmHg·min/L, P=0.03; drug groups at 3.4±2.1 vs. 1.7±0.9 mmHg·min/L, P=0.06). Before treatment began (D0), there were no statistical differences in vascular resistance index between the high-salt vehicle and high-salt drug groups (pre-occlusion 3.2±3.1 vs. 3.0±1.7 mmHg·min/L, P=0.83; post-occlusion 3.7±1.8 vs. 3.4±2.1 mmHg·min/L, P=0.78). In contrast, in the high-salt groups after 14 days of treatment, post-occlusion vascular resistance index in the drug-treated group was reduced by roughly 50% compared to the vehicle-treated group (1.5±0.4 vs. 3.2±1.0 mmHg·min/L, P=0.0003), with a similar reduction in pre-occlusion vascular resistance index (1.5±0.7 vs. 3.2±1.7 mmHg·min/L, P=0.008). Notably, in the high-salt drug group, there was a significant decrease in post-occlusion vascular resistance index from D0 to D14 (3.4±2.1 vs. 1.5±0.4

mmHg·min/L, P=0.003), again with a similar trend in pre-occlusion values (3.0±1.7 vs. 1.5±0.7 mmHg·min/L, P=0.04). Thus, the reduction in BP in hypertensive rats treated with GSNOR inhibitor was accompanied by a reduction in vascular resistance.

GSNOR inhibition restored FMD of Dahl-S hypertensive rats to the level of normotensive rats

To assess the effects of GSNOR inhibition on endothelial function in the hypertensive rats, FMD was measured at D0, D1, and D14 (Figure 5). The coefficient of variation for the low-salt vehicle group over time (calculated for individual rats over time and averaged) was 0.207. Similar to the BP results described above, FMD was normal in both low-salt groups, and impaired in the high-salt vehicle group (13.9±3.3% and 13.1±4.4% vs. 7.6±3.0%, P<0.05). Pairwise differences between groups on any given day did not reach significance, but FMD of all high-salt rats was significantly lower than that of all low-salt rats on D0, before treatment commenced (p=0.0027), confirming that FMD is impaired in Dahl-S rats on a high-salt diet. While GSNOR inhibitor treatment had no effect on FMD in the low-salt groups, it progressively and completely restored FMD to normal levels in the high-salt group between D0 and D14 (7.4±1.7% vs. 13.0±3.1%, P<0.001). No significant difference was observed between femoral artery basal diameters in the N6338 and vehicle high-salt groups (not shown). Furthermore, there were no differences in either aorta cGMP or plasma nitrite levels between N6338 and vehicle high-salt groups (not shown). Indexing of FMD to WSR reduced the level of significance but preserved the main effect, confirming that despite the functional defect in the microvasculature of the high-salt rats and its reversal by GSNOR inhibition, the conduit artery response to hyperemia was similarly impaired in the high-salt groups and reversed by GSNOR inhibition.

GSNOR inhibition prevented renal damage observed in hypertensive rats

At the end of the experiment, the rats were euthanized and the heart and kidneys from each rat were weighed. As shown in Fig. 6A, kidney weights were increased in the high-salt vehicle group (3.3±0.3 g) compared to weights in both low-salt groups (2.7±0.1 g and 2.6±0.2 g, $P<0.001$). GSNOR inhibition caused a trend toward lower kidney weights (2.9±0.3 g in the high-salt drug group vs. 3.3±0.3 g in the high-salt vehicle group, $P<0.05$). In contrast, there were no significant differences in heart weights (Fig. 6B) or body weights (not shown) among groups.

Histological assessment of kidneys showed that both low-salt groups had kidneys with normal glomerular and tubular architecture (Fig. 6C,D). Kidneys of high-salt rats showed significant tubular defects, whereas the glomeruli were mostly unaffected. All of these pathological conditions were substantially reduced in rats treated with N6338 as compared with vehicle (Fig. 6E,F), demonstrating that reversal of the pathological consequences of the Dahl-S hypertensive rat model by GSNOR inhibition was not limited to the cardiovascular system.

DISCUSSION

This study shows that the GSNOR inhibitor, N6338, preserves FMD under partial NOS inhibition, reduces BP and vascular resistance in hypertensive rats, and restores FMD in hypertensive rats from a substantially impaired state to that of normotensive rats. These results suggest that N6338 protects against both microvascular and conduit artery vasoactive dysfunction in a model of vascular inflammation and hypertension (27, 46), and that GSNOR inhibition may provide a strategy to increase bioavailable NO as a therapy for a number of vascular disorders (19). As NO has typically been linked to endothelial function through eNOS activity (*e.g.* FMD and eNOS are both impaired by cigarette smoke exposure in humans (3) and

eNOS gene therapy increases NO bioavailability and lowers BP in hypertensive rats (1, 44)), it is notable that FMD and BP can be altered by direct manipulation of NO storage pools rather than NO synthesis.

FMD measurement has been applied as a diagnostic tool in a range of physiological studies including vascular effects of intrinsic health factors and of environmental and behavioral influences on cardiovascular health (5, 13, 15, 16). The NO-dependency of FMD is demonstrable through inhibition of NOS (37). In our recently-developed rat FMD model, 8 mg/kg of L-NMMA was used to completely suppress FMD (17). In the present study, we have shown that 5 mg/kg L-NMMA induces acute partial suppression of FMD, which can be preserved if rats are pre-treated with N6338.

It is not clear why acutely depressed FMD, a process that requires active synthesis of NO by eNOS, was improved by N6338, which likely increased levels of pre-existing stores of NO. It is possible that under normal conditions, some of the NO generated acutely during reactive hyperemia is immediately consumed by processes other than those directly involved with relaxation of the affected artery. The FMD normally observed, therefore, may reflect the effect of residual acutely-generated NO. Because bioavailable NO is in equilibrium with both short-term NO-consuming processes and NO storage pools, including GSNO, increasing basal GSNO levels prior to eliciting FMD may pre-load the normal NO sinks that would otherwise consume NO generated acutely in response to reactive hyperemia. Hence, a higher net level of bioavailable NO may result during reactive hyperemia in the face of GSNOR inhibition than during normal GSNOR activity. The fact that N6338 did not increase FMD in the absence of L-NMMA may indicate that the NO pulse normally elicited by reactive hyperemia in our protocol elicits maximal artery dilation and further increasing bioavailable NO via GSNOR inhibition has

no effect. By contrast, the L-NMMA dose selected for our acute rat studies depressed hyperemia-induced NO below the level required to generate a maximal dilation response. Under this condition, GSNOR inhibition may increase bioavailable NO sufficiently to fully restore FMD despite co-existing partial inhibition of eNOS, as was observed. Our observation that L-NMMA inhibited the N6338-induced relaxation of pre-constricted aortic rings at only the lower N6338 concentrations tested further supports the importance of the stoichiometry between acutely-produced NO and the bioavailable NO pool. It is also notable that we observed substantial presence of GSNOR in the smooth muscle of arterioles and small arteries, suggesting that downstream elevation of bioavailable NO directly in the smooth muscle of arteries by GSNOR inhibition may compensate for possibly lower upstream production of NO by the endothelium.

Of perhaps greater importance is the observation that a probable chronic elevation of bioavailable NO, secondary to GSNOR inhibition, restores the magnitude of FMD in the Dahl-S hypertensive rat. This finding is consistent with reports that eNOS expression and endothelial-dependent relaxation are impaired in conduit arteries isolated from hypertensive Dahl-S rats (27, 45). Arterial β-adrenergic responsiveness is also decreased (34). Moreover, the high-salt diet may impair FMD directly, as even in healthy humans, a high-salt meal has been shown to reduce FMD in 30 minutes (10). Thus, FMD in hypertensive Dahl-S rats may be disrupted via intrinsic defects in conduit artery endothelial signaling that would otherwise lead to smooth muscle relaxation.

Sub-chronic GSNOR inhibition decreased femoral artery vascular resistance in high-salt Dahl-S rats compared to resistance in vehicle control high-salt rats under baseline conditions (pre-occlusion) and during reactive hyperemia (post-occlusion). Both of these observations have clinical relevance. Baseline vascular resistance primarily reflects basal microvascular tone, a

primary determinant of BP at rest. Our pre-occlusion vascular resistance data are consistent with the effects of chronic GSNOR inhibition on BP, which was substantially reduced. In contrast, peak reactive hyperemia is an index of maximum vasodilatory reserve, a functional parameter of importance to the brain and heart that normally operate at high oxygen extraction ratios. The capacity of these organs to respond to increased oxygen demand is highly dependent on increasing blood flow. Vasodilatory reserve indicates the upper limit of blood flow potentially available to these organs. Whereas reductions in vascular resistance primarily reflect the response of the femoral microvasculature to GSNOR inhibition, improvement in FMD reflects the conduit artery response to GSNOR inhibition.

The renin–angiotensin–aldosterone system and NADPH oxidase (39) within the kidney play important roles in the overall pathophysiology of renal disease through NF-κB-mediated upregulation of TGF-β (8, 46), MCP-1, and TNF-α (38, 46). These biochemical signals manifest as renal leukocyte recruitment, glomerular sclerosis, medullary fibrosis, poor renal hemodynamics, elevated BP, and proteinuria (38, 39). Pharmacological inhibition of NADPH oxidase results in decreased monocyte/macrophage infiltration and glomerular injury, and improved renal hemodynamics. Notably, GSNOR inhibition has been shown to inhibit NF-κB activation (32). Inhibition of NF-κB signaling has been observed upon treatment with NO donors such as sodium nitroprusside and GSNO, both which inhibit p65 binding to DNA promoter regions in cultured cells, resulting in down-regulation of NF-κB dependent gene expression (26). In other cell-based experiments, nitrosylation of the p50 subunit by the NO donor S-nitrosocysteine (the NO-bearing functional component of GSNO) also leads to inhibition of NF-κB DNA binding (24). GSNOR inhibitors of the same chemotype as N6338 cause both nitrosylation of the p65 subunit and decreased DNA binding activity (G.J.R. and S.C.M,

unpublished). Thus, prevention of kidney weight increase and damage by N6338 may be attributable, at least partly, to anti-inflammatory activity. Notably, moderately-old eNOS knock-out mice suffer from hypertension and renal injury that are exacerbated by high-salt diet (9), underscoring the connection between bioavailable NO and the control of these conditions.

It has recently been reported that complete absence of GSNOR in knock-out mice results in deficient DNA repair and increased propensity for tumorigenesis (25, 42). While there is a substantial difference between pharmacological inhibition of an enzyme and the life-long total absence of the protein, these results should be taken into consideration in the planning of initial clinical studies to ensure that such effects are prevented at the dosage used.

A limitation of this study is that the direct detection of N6338-induced changes in GSNOR activity *in vivo* is impractical because N6338 reversibly inhibits GSNOR. Therefore, disruption of tissues destroys the microenvironment within the cell and dilutes cellular contents, resulting in substantial dissociation of the inhibitor and restoration of enzymatic activity. Furthermore, direct measurement of endogenous GSNO levels is challenging and generally below levels of detection by current methods. However, GSNOR knock-out mice have demonstrated increased bioavailable NO as measured by heme-bound NO (22). By addition of GSNO to a cell-based SNO assay to increase SNO levels to within detectable range, we confirmed that N6338 increases SNOs in cultured cells, implicating GSNO preservation as a primary mechanism of N6338's effects in a biological system. Taken together, the *in vivo* effects of treatment with GSNOR inhibitor N6338, paired with evidence of GSNOR inhibition from our *in vitro* experiments, strongly suggest that GSNOR inhibition led to an increase in NO-mediated signaling that cumulatively improved cardiovascular hemodynamics and renal pathology in this study.

In summary, using an approach that we developed to measure FMD in living rats, we have shown that a small molecule inhibitor of GSNOR improves FMD and lowers BP and vascular resistance in rat models of vascular disease. GSNOR inhibition, by this or other small molecules, may therefore hold potential for clinical treatment of disease states characterized by vascular and renal inflammation and endothelial dysfunction.

ACKNOWLEDGEMENTS

We thank Christian Heiss for helpful discussion, Michael Suniga and Kirsten Look for technical assistance, Limin Liu for supplying embryonic fibroblasts, and Vivian Weinberg, Xiaoyin Wang, and Kirstin Aschbacher for statistical assistance.

FUNDING SOURCES

This work was supported by a fellowship from the Margoes Foundation/UCSF Cardiovascular Research Institute to Q.C. and by NIH grant R01 HL086917 and sponsored research support from N30 Pharmaceuticals to M.L.S.

DISCLOSURES

This study was funded in part through a research collaboration with N30 Pharmaceuticals. A.K.P., C.S.D., S.C.M., J.P.B., G.P.D, and G.J.R. are or have been employed by N30.

REFERENCES

1. **Alexander MY, Brosnan MJ, Hamilton CA, Fennell JP, Beattie EC, Jardine E, Heistad DD, and Dominiczak AF**. Gene transfer of endothelial nitric oxide synthase but not

524 Cu/Zn superoxide dismutase restores nitric oxide availability in the SHRSP. *Cardiovasc Res* 47:
525 609-617, 2000.
526 2. **Anderson TJ, Uehata A, Gerhard MD, Meredith IT, Knab S, Delagrange D,**
527 **Lieberman EH, Ganz P, Creager MA, Yeung AC, and Selwyn AP**. Close relation of
528 endothelial function in the human coronary and peripheral circulations. *J Am Coll Cardiol* 26:
529 1235-1241, 1995.
530 3. **Barua RS, Ambrose JA, Eales-Reynolds LJ, DeVoe MC, Zervas JG, and Saha DC**.
531 Dysfunctional endothelial nitric oxide biosynthesis in healthy smokers with impaired
532 endothelium-dependent vasodilatation. *Circulation* 104: 1905-1910, 2001.
533 4. **Beigi F, Gonzalez DR, Minhas KM, Sun QA, Foster MW, Khan SA, Treuer AV,**
534 **Dulce RA, Harrison RW, Saraiva RM, Premer C, Schulman IH, Stamler JS, and Hare JM**.
535 Dynamic denitrosylation via S-nitrosoglutathione reductase regulates cardiovascular function.
536 *Proc Natl Acad Sci U S A* 109: 4314-4319, 2012.
537 5. **Celermajer DS, Sorensen KE, Georgakopoulos D, Bull C, Thomas O, Robinson J,**
538 **and Deanfield JE**. Cigarette smoking is associated with dose-related and potentially reversible
539 impairment of endothelium-dependent dilation in healthy young adults. *Circulation* 88: 2149-
540 2155, 1993.
541 6. **Celermajer DS, Sorensen KE, Gooch VM, Spiegelhalter DJ, Miller OI, Sullivan ID,**
542 **Lloyd JK, and Deanfield JE**. Non-invasive detection of endothelial dysfunction in children and
543 adults at risk of atherosclerosis. *Lancet* 340: 1111-1115, 1992.
544 7. **Chemla D, Antony I, Zamani K, and Nitenberg A**. Mean aortic pressure is the
545 geometric mean of systolic and diastolic aortic pressure in resting humans. *J Appl Physiol* 99:
546 2278-2284, 2005.

8. **Dahly AJ, Hoagland KM, Flasch AK, Jha S, Ledbetter SR, and Roman RJ**. Antihypertensive effects of chronic anti-TGF-beta antibody therapy in Dahl S rats. *Am J Physiol Regul Integr Comp Physiol* 283: R757-767, 2002.

9. **Daumerie G, Bridges L, Yancey S, Davis W, Huang P, Loscalzo J, and Pointer MA**. The effect of salt on renal damage in eNOS-deficient mice. *Hypertens Res* 33: 170-176, 2010.

10. **Dickinson KM, Clifton PM, and Keogh JB**. Endothelial function is impaired after a high-salt meal in healthy subjects. *Am J Clin Nutr* 93: 500-505, 2011.

11. **Flammer AJ, Anderson T, Celermajer DS, Creager MA, Deanfield J, Ganz P, Hamburg NM, Luscher TF, Shechter M, Taddei S, Vita JA, and Lerman A**. The assessment of endothelial function: from research into clinical practice. *Circulation* 126: 753-767, 2012.

12. **Foster MW, McMahon TJ, and Stamler JS**. S-nitrosylation in health and disease. *Trends Mol Med* 9: 160-168, 2003.

13. **Ghiadoni L, Huang Y, Magagna A, Buralli S, Taddei S, and Salvetti A**. Effect of acute blood pressure reduction on endothelial function in the brachial artery of patients with essential hypertension. *J Hypertens* 19: 547-551, 2001.

14. **Green D**. Point: Flow-mediated dilation does reflect nitric oxide-mediated endothelial function. *J Appl Physiol* 99: 1233-1234; discussion 1237-1238, 2005.

15. **Heiss C, Jahn S, Taylor M, Real WM, Angeli FS, Wong ML, Amabile N, Prasad M, Rassaf T, Ottaviani JI, Mihardja S, Keen CL, Springer ML, Boyle A, Grossman W, Glantz SA, Schroeter H, and Yeghiazarians Y**. Improvement of endothelial function with dietary flavanols is associated with mobilization of circulating angiogenic cells in patients with coronary artery disease. *J Am Coll Cardiol* 56: 218-224, 2010.

16. **Heiss C, Schanz A, Amabile N, Jahn S, Chen Q, Wong ML, Rassaf T, Heinen Y, Cortese-Krott M, Grossman W, Yeghiazarians Y, and Springer ML**. Nitric oxide synthase expression and functional response to nitric oxide are both important modulators of circulating angiogenic cell response to angiogenic stimuli. *Arterioscler Thromb Vasc Biol* 30: 2212-2218, 2010.

17. **Heiss C, Sievers RE, Amabile N, Momma TY, Chen Q, Natarajan S, Yeghiazarians Y, and Springer ML**. In vivo measurement of flow-mediated vasodilation in living rats using high-resolution ultrasound. *Am J Physiol Heart Circ Physiol* 294: H1086-1093, 2008.

18. **Jensen DE, Belka GK, and Du Bois GC**. S-Nitrosoglutathione is a substrate for rat alcohol dehydrogenase class III isoenzyme. *Biochem J* 331 (Pt 2): 659-668, 1998.

19. **Leopold JA, and Loscalzo J**. New developments in nitrosovasodilator therapy. *Vasc Med* 2: 190-202, 1997.

20. **Lima B, Forrester MT, Hess DT, and Stamler JS**. S-nitrosylation in cardiovascular signaling. *Circ Res* 106: 633-646, 2010.

21. **Lima B, Lam GK, Xie L, Diesen DL, Villamizar N, Nienaber J, Messina E, Bowles D, Kontos CD, Hare JM, Stamler JS, and Rockman HA**. Endogenous S-nitrosothiols protect against myocardial injury. *Proc Natl Acad Sci U S A* 106: 6297-6302, 2009.

22. **Liu L, Hausladen A, Zeng M, Que L, Heitman J, and Stamler JS**. A metabolic enzyme for S-nitrosothiol conserved from bacteria to humans. *Nature* 410: 490-494, 2001.

23. **Liu L, Yan Y, Zeng M, Zhang J, Hanes MA, Ahearn G, McMahon TJ, Dickfeld T, Marshall HE, Que LG, and Stamler JS**. Essential roles of S-nitrosothiols in vascular homeostasis and endotoxic shock. *Cell* 116: 617-628, 2004.

591 24. **Marshall HE, and Stamler JS**. Inhibition of NF-kappa B by S-nitrosylation.
592 *Biochemistry* 40: 1688-1693, 2001.
593 25. **Ozawa K, Tsumoto H, Wei W, Tang CH, Komatsubara AT, Kawafune H, Shimizu**
594 **K, Liu L, and Tsujimoto G**. Proteomic analysis of the role of S-nitrosoglutathione reductase in
595 lipopolysaccharide-challenged mice. *Proteomics* 12: 2024-2035, 2012.
596 26. **Paradkar PN, and Roth JA**. Nitric oxide transcriptionally down-regulates specific
597 isoforms of divalent metal transporter (DMT1) via NF-kappaB. *J Neurochem* 96: 1768-1777,
598 2006.
599 27. **Quaschning T, D'Uscio LV, Shaw S, Grone HJ, Ruschitzka F, and Luscher TF**.
600 Vasopeptidase inhibition restores renovascular endothelial dysfunction in salt-induced
601 hypertension. *J Am Soc Nephrol* 12: 2280-2287, 2001.
602 28. **Que LG, Liu L, Yan Y, Whitehead GS, Gavett SH, Schwartz DA, and Stamler JS**.
603 Protection from experimental asthma by an endogenous bronchodilator. *Science* 308: 1618-1621,
604 2005.
605 29. **Que LG, Yang Z, Stamler JS, Lugogo NL, and Kraft M**. S-nitrosoglutathione
606 reductase: an important regulator in human asthma. *Am J Respir Crit Care Med* 180: 226-231,
607 2009.
608 30. **Rosenthal GJ, Blonder J, Damaj B, Richards J, Elia M, and Scoggin C**. A novel
609 compound that inhibits S−nitrosoglutathione reductase protects against experimental asthma
610 [abstract]. 179;2009:A4151.
611 31. **Rudolph V, and Freeman BA**. Cardiovascular consequences when nitric oxide and lipid
612 signaling converge. *Circ Res* 105: 511-522, 2009.

613 32. **Sanghani PC, Davis WI, Fears SL, Green SL, Zhai L, Tang Y, Martin E, Bryan NS,**
614 **and Sanghani SP**. Kinetic and cellular characterization of novel inhibitors of S-
615 nitrosoglutathione reductase. *J Biol Chem* 284: 24354-24362, 2009.
616 33. **Sessa WC**. Molecular control of blood flow and angiogenesis: role of nitric oxide. *J*
617 *Thromb Haemost* 7 Suppl 1: 35-37, 2009.
618 34. **Soltis EE, and Katovich MJ**. Reduction in aortic smooth muscle beta-adrenergic
619 responsiveness results in enhanced norepinephrine responsiveness in the Dahl salt-sensitive rat.
620 *Clin Exp Hypertens A* 13: 117-132, 1991.
621 35. **Sun J, and Murphy E**. Protein S-nitrosylation and cardioprotection. *Circ Res* 106: 285-
622 296, 2010.
623 36. **Sun X, Wasley J, Qiu J, Blonder J, Stout A, Green L, Strong S, Colagiovanni D,**
624 **Richards J, Mutka S, Chun L, and Rosenthal G**. Discovery of S-nitrosoglutathione reductase
625 inhibitors: Potential agents for the treatment of asthma and other inflammatory diseases. *ACS*
626 *Med Chem Lett* 2: 402-406, 2011.
627 37. **Thijssen DH, Black MA, Pyke KE, Padilla J, Atkinson G, Harris RA, Parker BA,**
628 **Widlansky ME, Tschakovsky ME, and Green DJ**. Assessment of flow mediated dilation
629 (FMD) in humans: a methodological and technical guideline. *Am J Physiol Heart Circ Physiol*
630 300: H2-H12, 2011.
631 38. **Tian N, Moore RS, Braddy S, Rose RA, Gu JW, Hughson MD, and Manning RD,**
632 **Jr.** Interactions between oxidative stress and inflammation in salt-sensitive hypertension. *Am J*
633 *Physiol* 293: H3388-3395, 2007.

634 39. **Tian N, Moore RS, Phillips WE, Lin L, Braddy S, Pryor JS, Stockstill RL, Hughson**
635 **MD, and Manning RD, Jr.** NADPH oxidase contributes to renal damage and dysfunction in
636 Dahl salt-sensitive hypertension. *Am J Physiol* 295: R1858-1865, 2008.
637 40. **Vita JA, and Keaney JF, Jr.** Endothelial function: a barometer for cardiovascular risk?
638 *Circulation* 106: 640-642, 2002.
639 41. **Walford G, and Loscalzo J**. Nitric oxide in vascular biology. *J Thromb Haemost* 1:
640 2112-2118, 2003.
641 42. **Wei W, Li B, Hanes MA, Kakar S, Chen X, and Liu L**. S-nitrosylation from GSNOR
642 deficiency impairs DNA repair and promotes hepatocarcinogenesis. *Sci Transl Med* 2: 19ra13,
643 2010.
644 43. **Yang Y, and Loscalzo J**. S-nitrosoprotein formation and localization in endothelial cells.
645 *Proc Natl Acad Sci U S A* 102: 117-122, 2005.
646 44. **Zhao CX, Xu X, Cui Y, Wang P, Wei X, Yang S, Edin ML, Zeldin DC, and Wang**
647 **DW**. Increased endothelial nitric-oxide synthase expression reduces hypertension and
648 hyperinsulinemia in fructose-treated rats. *J Pharmacol Exp Ther* 328: 610-620, 2009.
649 45. **Zhou MS, Kosaka H, Tian RX, Abe Y, Chen QH, Yoneyama H, Yamamoto A, and**
650 **Zhang L**. L-Arginine improves endothelial function in renal artery of hypertensive Dahl rats. *J*
651 *Hypertens* 19: 421-429, 2001.
652 46. **Zhu A, Yoneda T, Demura M, Karashima S, Usukura M, Yamagishi M, and Takeda**
653 **Y**. Effect of mineralocorticoid receptor blockade on the renal renin-angiotensin system in Dahl
654 salt-sensitive hypertensive rats. *J Hypertens* 27: 800-805, 2009.
655
656

FIGURE LEGENDS:

Fig. 1. GSNOR inhibition, localization, and activity. (A) N6338 caused dose-dependent and potent inhibition of human GSNOR activity *in vitro*. Graph represents one experiment using duplicate samples at each dose tested. (B) N6338 increased SNO levels in mouse embryonic fibroblasts. Mean SNO levels ± SEM are shown (n=12 independent wells per group; $P<0.0001$, two-tailed t-test). (C-G) GSNOR protein was evident in human and rat cardiovascular tissue by immunohistochemistry: (C) IgG negative control or (D) human-specific GSNOR antibody staining predominantly in the smooth muscle of a myocardial arteriole or small artery in human heart, and (E) predominantly in the endothelium of a human myocardial venule; (F) IgG negative control or (G) rat-specific GSNOR antibody staining predominantly in the smooth muscle of an arteriole in rat heart. In all micrographs, scale bars = 50 μm, asterisks denote vessel lumens, blue arrows show smooth muscle, and red arrows show endothelium. (H) GSNOR activity was present in rat heart and aorta, and inhibited by N6338 when this compound was added *in vitro*. Activity was measured in the absence (white bars) or presence of 1 μM (gray bars) or 10 μM (black bars) N6338. Bars are mean±SD of tissues from 4 rats. (I) N6338 caused dose-dependent relaxation in rat aortic rings precontracted with phenylephrine. This relaxation by N6338 was significantly attenuated by pretreatment of rings with 10 μM ODQ, 100 μM L-NMMA, or 300 μM carboxy PTIO for 30 min prior to N6338 administration. Values are mean±SEM of 4 rings/group.

Fig. 2. Effect of GSNOR inhibitor on acute impairment of FMD. Pilot experiments showed that roughly half-maximal inhibition of FMD occurs 15 min after 5 mg/kg, i.v. L-NMMA. We

pretreated rats with this dose of L-NMMA before eliciting FMD responses. Prior treatment (24 h, i.v.) with 10 mg/kg N6338 (n=7), but not PBS (n=7), preserved FMD in L-NMMA-treated rats in a cross-over study design. FMD is shown both as raw data and indexed to WSR. Values are mean±SD.

Fig. 3. Effect of GSNOR inhibitor on BP in hypertensive rats. (A) BP measurements in anesthetized rats. n=6 for each normotensive group; n=7 for each hypertensive group; $P<0.05$ for overall effect. (B) BP measurements in conscious rats. N6338 reversed an increase in BP in the hypertensive rats (n=10). *$p<0.001$ high-salt vehicle (n=7) vs. high-salt drug (n=10). Values are mean±SD. Note that diastolic BP measurements by tail-cuff methodology are approximations and are included here for reference, while systolic values represent true measurements.

Fig. 4. Effect of GSNOR inhibitor on vascular resistance. Vascular resistance index was increased with high-salt diet, and N6338 reduced the vascular resistance index after two weeks of treatment. Values are mean±SD. * = significant at adjusted alpha error rate of 0.0041 for multiple comparisons.

Fig. 5. Effect of GSNOR inhibitor on FMD in hypertensive rats. FMD was substantially impaired in the hypertensive rats. N6338 fully restored FMD over the two-week treatment period to levels seen in normotensive control rats. FMD is shown both as raw data and indexed to WSR. The comparisons between individual groups did not reach significance, although significance was reached for the overall effect with $p<0.05$. The difference in FMD in all high-salt rats vs. all low-salt rats at D0 was significant ($p=0.0027$, t-test). The change from D0 to D14 in the high-salt

703 drug group was significant in both analyses (*p<0.001 D0 vs. D14). Values are mean±SD.

704

705 Fig. 6. Effect of GSNOR inhibitor on the kidneys. (A) At D14, kidney weights were increased in
706 the high-salt vehicle group, while weights in the high-salt drug group trended lower. Values are
707 mean±SD. (B) There were no significant differences in heart weights among treatments. (C)
708 Low-salt vehicle and (D) low-salt drug groups: Histology of renal cortex shows normal
709 glomerular (arrows) and tubular architecture (arrowheads) with back-to-back tubules, no
710 interstitial edema, and intact tubular basement membrane; with no detectable difference between
711 these low-salt groups. (E) High-salt vehicle group: In contrast, histology of renal cortices shows
712 significant tubular swelling and dilation (asterisk), interstitial edema, loss of tubular brush
713 borders, and basement membrane disruption (arrowheads), all of which were substantially
714 reduced in rats treated with N6338 (F). Scale bar = 50 μm.

715 Table 1. Exact BP measurements corresponding to Figure 3A (isoflurane anesthesia)
716

	Treatment day			
Group	D0	D4	D9	D14
Low-salt vehicle	83.9±7.8/ 65.2±4.9	87.8±3.1/ 67.1±3.1	86.8±3.1/ 66.6±2.7	86.7±5.4/ 64.3±5.3
Low-salt drug	86.0±5.4/ 66.2±4.2	84.9±7.0/ 65.7±5.9	84.4±3.5/ 65.3±2.5	85.6±4.2/ 64.6±3.5
High-salt vehicle	112.2±12.9/ 88.5±10.9	117.9±16.8/ 93.8±15.7	122.8±16.5/ 100.1±16.2	125.0±14.6/ 98.4±13.7
High-salt drug	121.7±14.7/ 103.2±15.3	108.3±18.7/ 87.6±19.4	98.3±6.7/ 77.5±7.2	97.4±6.0/ 75.8±8.1

717

718 Values are systolic/diastolic BP (mmHg) expressed as mean±SD.

719
720

721 Table 2. Exact BP measurements corresponding to Figure 3B (conscious)
722

	Treatment				
	Low Salt		High Salt		
Group		D 0	D 4	D 9	D14
Vehicle	129.8±4.0/	197.9±3.5/	197.8±3.4/	199.6±4.9/	203.8±1.9/
	85.1±4.6	142.6±2.6	148.1±4.0	141.2±2.8	143.7±7.5
Drug	123.9±4.2/	200.8±6.6/	184.4±6.7/	171.8±5.0/	170.0±5.3/
	87.8±4.0	141.8±5.8	126.8±5.2	124.4±2.6	122.7±6.4

723

724 Values are systolic/diastolic BP (mmHg) expressed as mean±SD.

725

726
727

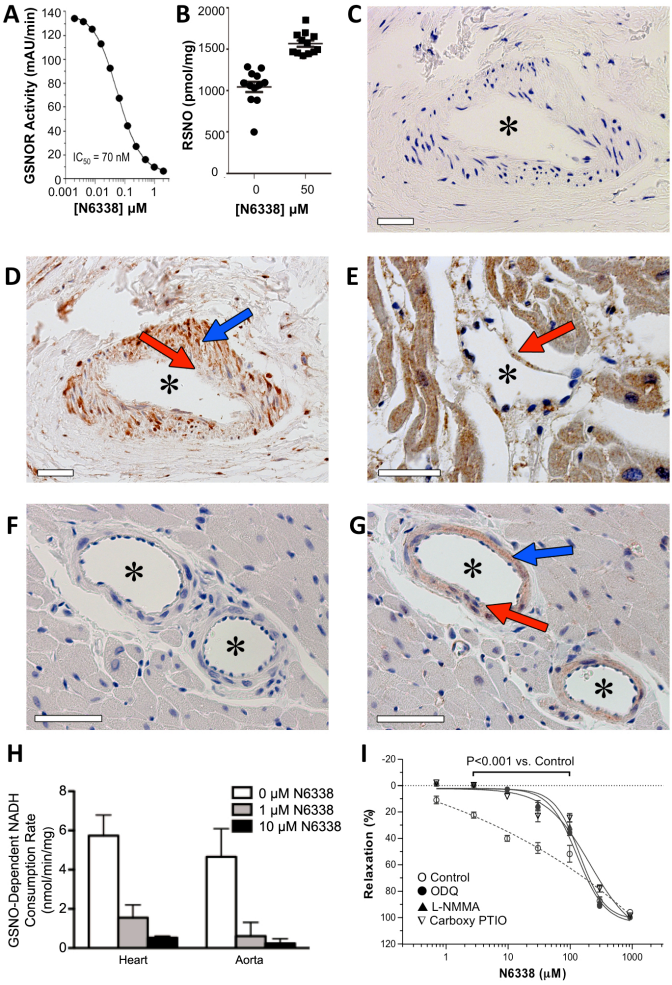
A
GSNOR Activity (mAU/min)
140
120
100
80
60
40
20
0
IC50 = 70 nM
0.001
0.01
0.1
1
[N6338] µM
B
RSNO (pmol/mg)
2000
1500
1000
500
0
0
50
[N6338] µM
C
D
E
F
G
H
GSNO-Dependent NADH Consumption Rate (nmol/min/mg)
8
6
4
2
0
0 µM N6338
1 µM N6338
10 µM N6338
Heart
Aorta
I
P<0.001 vs. Control
Relaxation (%)
-20
0
20
40
60
80
100
120
O Control
● ODQ
▲ L-NMMA
▽ Carboxy PTIO
1
10
100
1000
N6338 (µM)

Figure 1

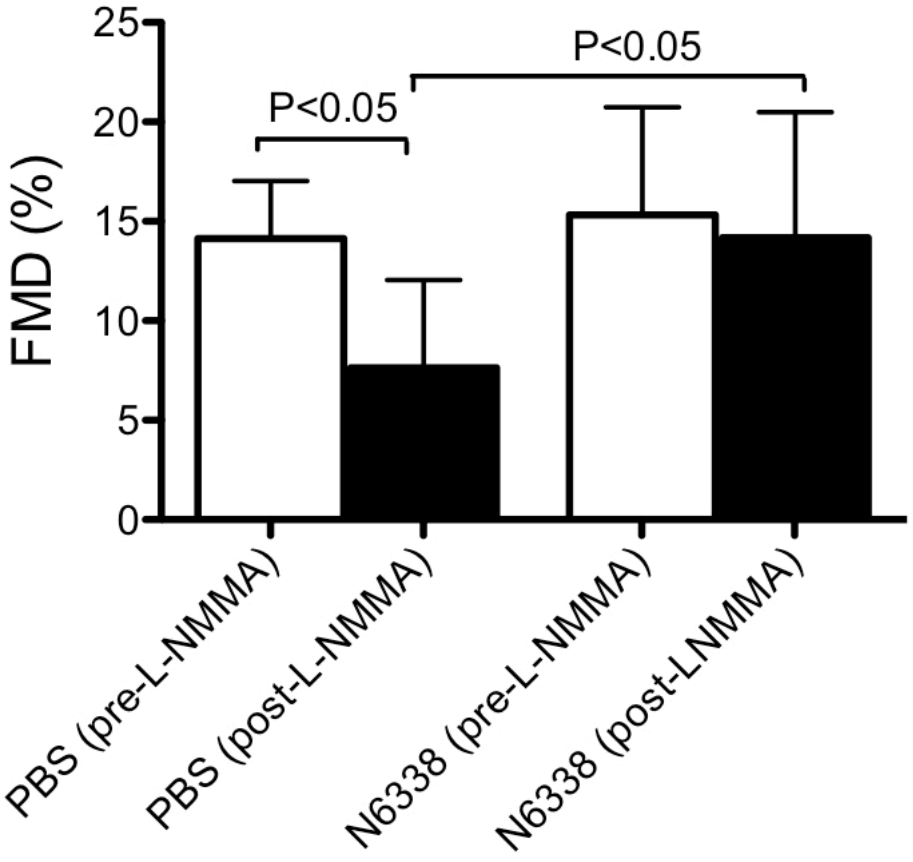
FMD (%)
25
20
15
10
5
0
P<0.05
P<0.05
PBS (pre-L-NMMA)
PBS (post-L-NMMA)
N6338 (pre-L-NMMA)
N6338 (post-LNMMA)

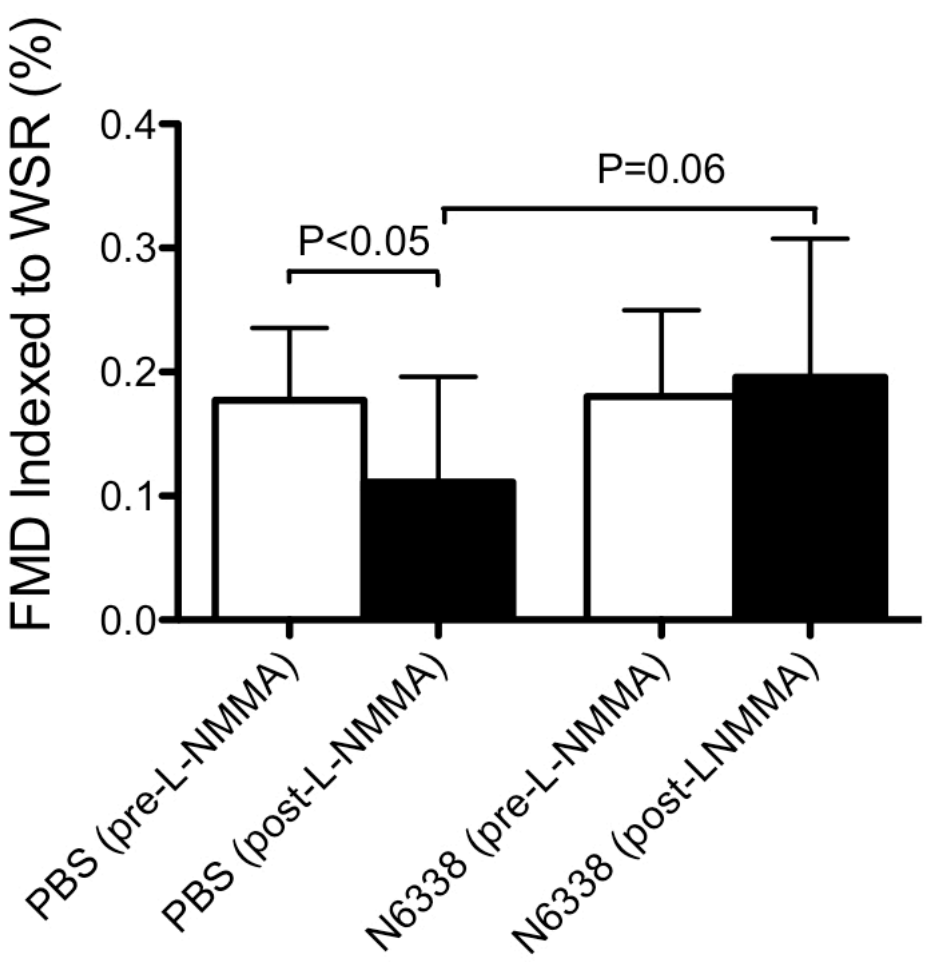
FMD Indexed to WSR (%)
0.4
0.3
0.2
0.1
0.0
P=0.06
P<0.05
PBS (pre-L-NMMA)
PBS (post-L-NMMA)
N6338 (pre-L-NMMA)
N6338 (post-LNMMA)

Figure 2

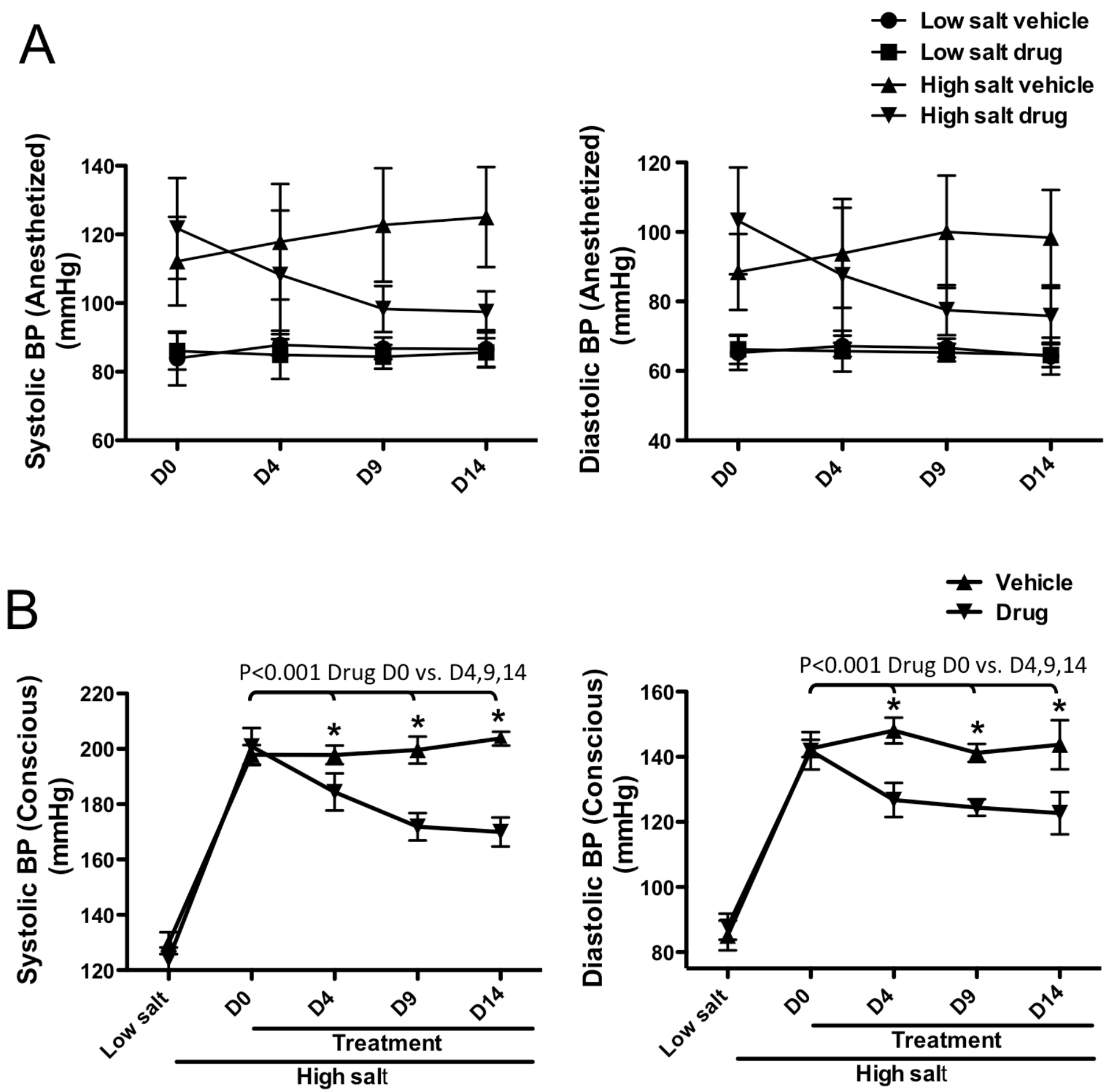
A
Low salt vehicle
Low salt drug
High salt vehicle
High salt drug
Systolic BP (Anesthetized) (mmHg)
140
120
100
80
60
D0
D4
D9
D14
Diastolic BP (Anesthetized) (mmHg)
120
100
80
60
40
D0
D4
D9
D14
B
Vehicle
Drug
Systolic BP (Conscious) (mmHg)
P<0.001 Drug D0 vs. D4,9,14
220
200
180
160
140
120
*
*
*
Low salt
D0
D4
D9
D14
Treatment
High salt
Diastolic BP (Conscious) (mmHg)
P<0.001 Drug D0 vs. D4,9,14
160
140
120
100
80
*
*
*
Low salt
D0
D4
D9
D14
Treatment
High salt

Figure 3

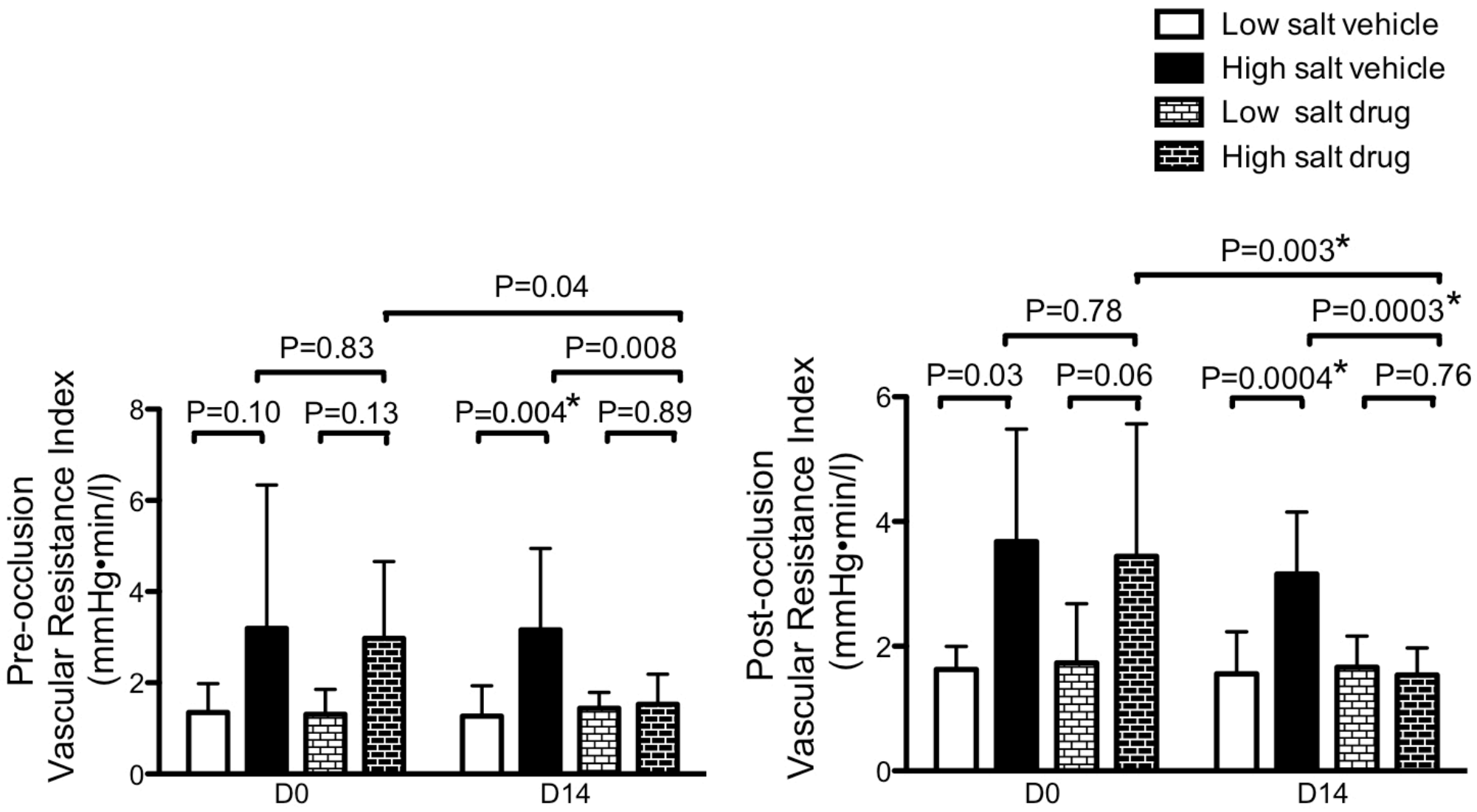
Low salt vehicle
High salt vehicle
Low salt drug
High salt drug
Pre-occlusion
Vascular Resistance Index
(mmHg•min/l)
P=0.04
P=0.83
P=0.008
P=0.10
P=0.13
P=0.004*
P=0.89
0
2
4
6
8
D0
D14
Post-occlusion
Vascular Resistance Index
(mmHg•min/l)
P=0.003*
P=0.78
P=0.0003*
P=0.03
P=0.06
P=0.0004*
P=0.76
0
2
4
6
D0
D14

Figure 4

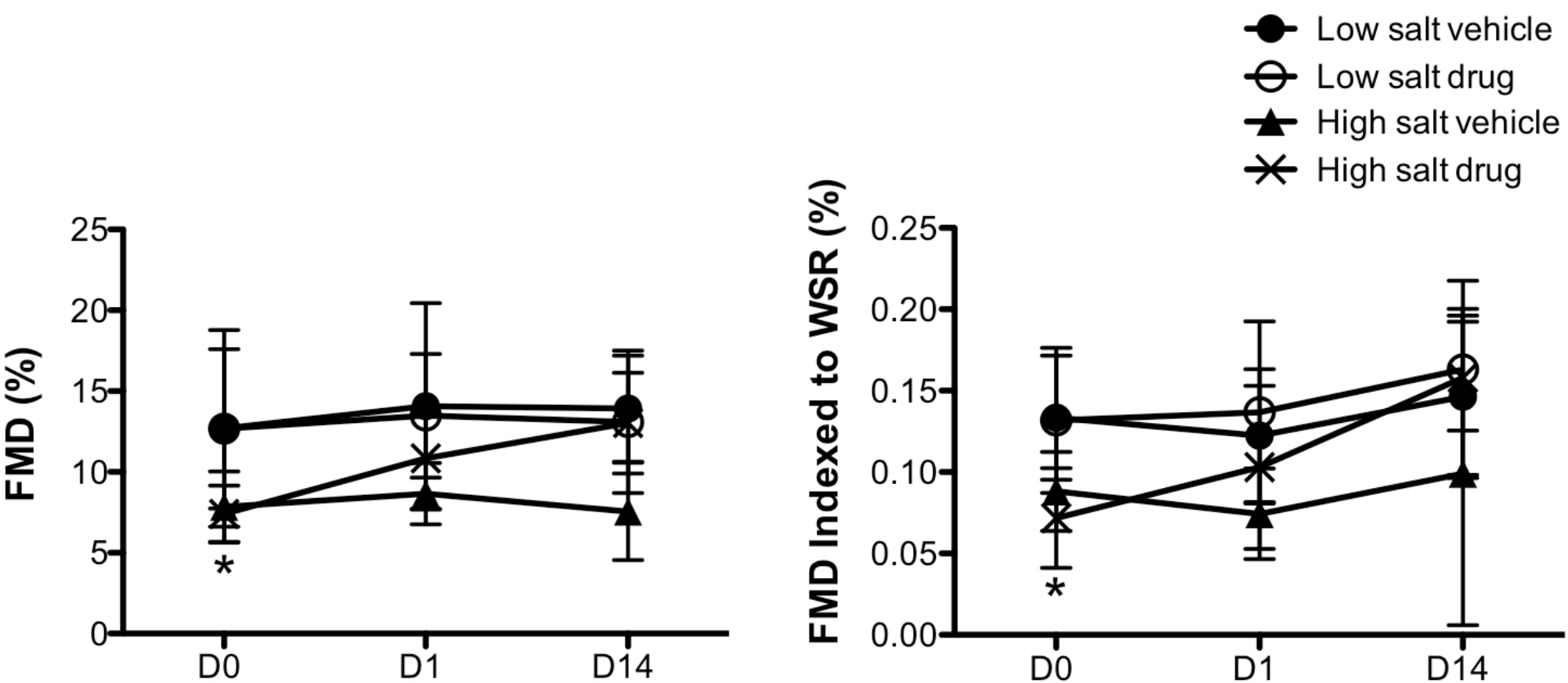
Low salt vehicle
Low salt drug
High salt vehicle
High salt drug
FMD (%)
25
20
15
10
5
0
D0
D1
D14
*
FMD Indexed to WSR (%)
0.25
0.20
0.15
0.10
0.05
0.00
D0
D1
D14
*

Figure 5

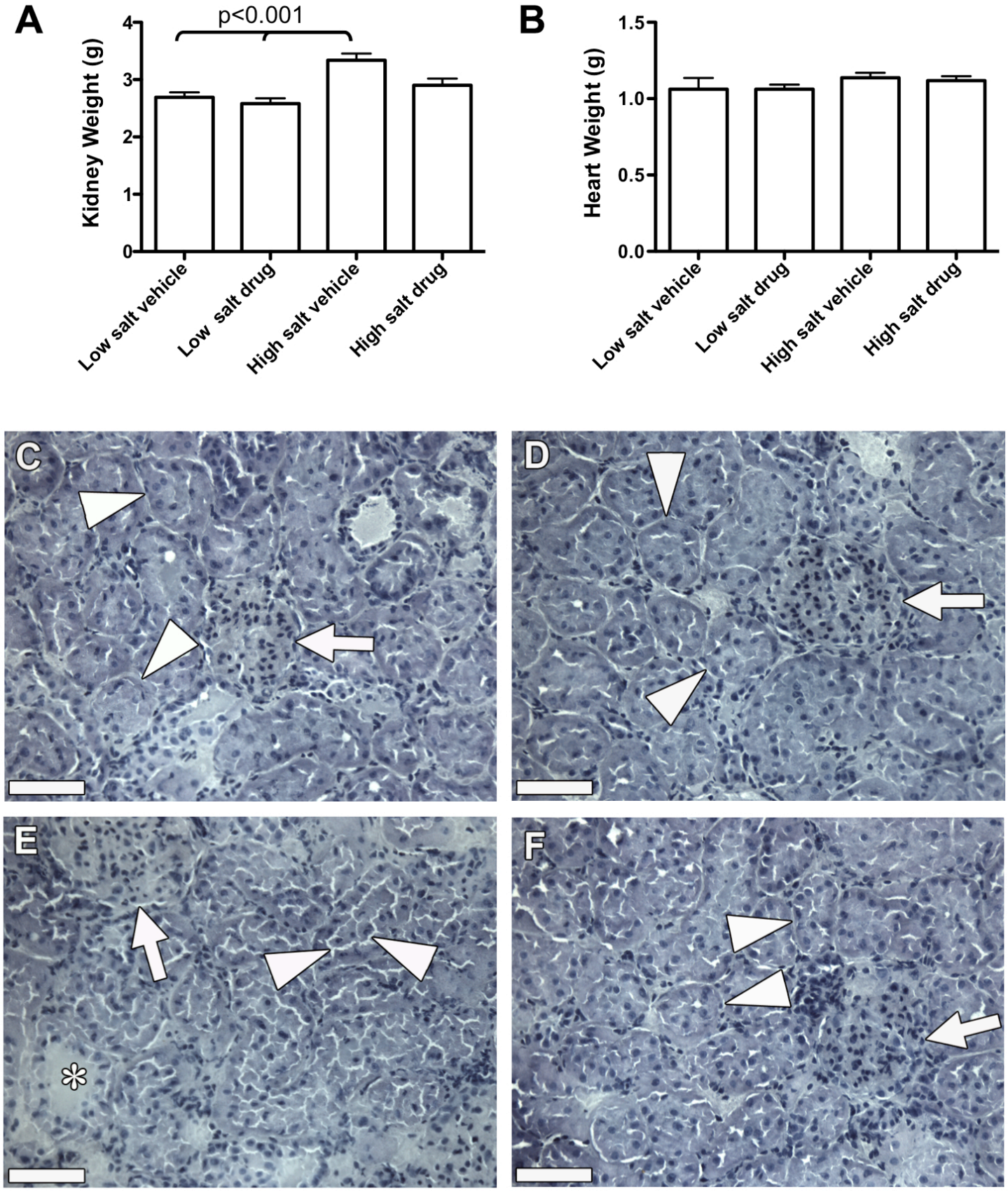
A
p<0.001
Kidney Weight (g)
0
1
2
3
4
Low salt vehicle
Low salt drug
High salt vehicle
High salt drug
B
Heart Weight (g)
0.0
0.5
1.0
1.5
Low salt vehicle
Low salt drug
High salt vehicle
High salt drug
C
D
E
F

Figure 6